Fluo-8® Calcium Reagents and Screen Quest™ Fluo-8 NW Calcium Assay Kits

I. Introduction

Calcium acts as a universal second messenger in a variety of cells. The beginning of life, the act of fertilization, is regulated by Ca^{2+}. Numerous functions of all types of cells are regulated by Ca^{2+} to a greater or lesser degree. Since the 1920s, scientists have attempted to measure Ca^{2+}, but few were successful due to limited availability of Ca^{2+} probes. The first reliable measurements of Ca^{2+} were performed by Ridgway and Ashley by injecting the photoprotein aequorin into the giant muscle fiber of the barnacle. Subsequently, in the 1980s, Tsien and colleagues produced a variety of fluorescent indicators. Among them the fluorescein-based Ca^{2+} reagents (such as Fluo-3 and Fluo-4) have provided trustworthy methods for measuring Ca^{2+}. Since the development of these Ca^{2+} probes, investigations of Ca^{2+}-related intracellular phenomena have skyrocketed.

II. Fluo-8® Calcium Indicators, the Brightest Calcium Dyes

Since being introduced, Fluo-3 imaging and its analogs (such as Fluo-4) have revealed the spatial dynamics of many elementary processes in Ca^{2+} signaling. Fluo-3 and Fluo-4 have also been extensively used for flow cytometry and microplate-based (such as FLIPR™) calcium detections. However, the weak signal and harsh dye-loading conditions have limited their applications in some cellular analysis. Our Fluo-8® serial calcium detection reagents have been developed to address these limitations of Fluo-3 and Fluo-4.

The most important properties of Fluo-3 and Fluo-4 in cellular applications are their absorption spectrum compatible with excitation at 488 nm by argon-ion laser sources, and a very large fluorescence intensity increase in response to Ca^{2+} binding. These two valuable properties have been retained intact with our Fluo-8® Ca^{2+} detection reagents. The absorption and emission peaks of Fluo-8® reagents are 490 nm and 514 nm, respectively. They can be well excited with an argon ion laser at 488 nm, and their emitted fluorescence (at wavelength 514 nm) increases with increasing Ca^{2+}. Fluo-8® is determined to undergo a > 200-fold increase in fluorescence upon binding to Ca^{2+}. Because the range of increase in Ca^{2+} in many cells after stimulation is generally 5- to10-fold, Fluo-8® is an excellent probe to use with high sensitivity in this region. The K_d of Fluo-8® is estimated to be 389 nM (22 °C, pH 7.0–7.5), but this value may be significantly influenced by pH, viscosity, and binding proteins *in vivo* conditions.

Besides their convenient 488 nm excitation wavelength and large fluorescence enhancement by calcium, Fluo-8® is much brighter in cells than Fluo-3 and Fluo-4 as shown in Figure 1. In addition, Fluo-8® is much more readily loaded into live cells than Fluo-3 and Flu-4, both of which require 37 °C for optimal cell loading. Fluo-8® reagents have a less temperature-dependent cell loading property, giving similar results either at room temperature or 37 °C. This characteristic makes Fluo-8® more robust for HTS applications.

Table 1. Spectral and Ca^{2+}–Binding Properties of Fluo-8® Calcium Detection Reagents

Ca^{2+} Indicator	Excitation	Emission	K_d of Ca^{2+}-Binding
Fluo-8®	490 nm	514 nm	389 nM
Fluo-8H™	490 nm	514 nm	232 nM
Fluo-8L™	490 nm	514 nm	1.86 uM

Compared to Fluo-3 and Fluo-4, our Fluo-8® calcium detection reagents have the following advantages:

- *Convenient Wavelengths:* maximum excitation @ ~490 nm; maximum emission @ ~514 nm.
- *Enhanced Intensity:* 2 times brighter than Fluo-4 AM; 4 times brighter than Fluo-3 AM.
- *Faster Loading:* dye loading at room temperature (rather than 37 ºC that is required for Fluo-4 AM).
- *Versatile Ca^{2+}-Binding K_d* as shown in Table 1.
- *Versatile Packing Sizes to Meet Your Special Needs*: 1 mg; 10x50 µg; 20x50 µg; HTS packages.

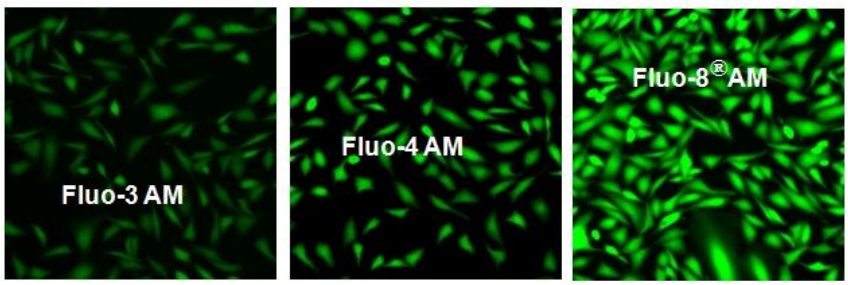

Figure 1. U2OS cells were seeded overnight at 40,000 cells/100 µL/well in a 96-well black wall/clear bottom costar plate. The growth medium was removed, and the cells were incubated with, respectively, 100 µL of Fluo-3 AM, Fluo-4 AM and Fluo-8® AM in HHBS at a concentration of 4 uM in a 37 °C, 5% CO_2 incubator for 1 hour. The cells were washed twice with 200 µL HHBS, then imaged with a fluorescence microscope (Olympus IX71) using FITC channel.

Ordering: sales@aatbio.com; Tel: 800-990-8053 or 408-733-1055; Fax: 408-733-1304
Technical Support: support@aatbio.com; Tel: 408-733-1055

III. Use of Fluo-8® AM Esters

1. Load Cells with Fluo-8® AM Esters:

AM esters are the non-polar esters that readily cross live cell membranes, and rapidly hydrolyzed by cellular esterases inside live cells. AM esters are widely used for loading a variety of polar fluorescent probes into live cell non-invasively. However, cautions must be excised when AM esters are used since they are susceptible to hydrolysis, particularly in solution. They should be reconstituted just before use in high-quality, anhydrous dimethylsulfoxide (DMSO). DMSO stock solutions may be stored desiccated at –20 °C and protected from light. Under these conditions, AM esters should be stable for several months.

Following is our recommended protocol for loading Fluo-8® AM esters into live cells. This protocol only provides a guideline, and should be modified according to your specific needs.

a) Prepare a 2 to 5 mM stock solution of Fluo-8® AM esters in high-quality, anhydrous DMSO.

b) On the day of the experiment, either dissolve Fluo-8® in DMSO or thaw an aliquot of the indicator stock solution to room temperature. Prepare a working solution of 1 to 10 µM in Hanks and Hepes buffer (HHBS) or the buffer of your choice with 0.02% *Pluronic® F-127*. For most of cell lines, Fluo-8® reagents with a concentration ranging from 4-5 uM are recommended. The exact concentration of the indicator required for cell loading must be determined empirically. To avoid any artifacts caused by overloading and potential dye toxicity, it is recommended to use the minimal dye concentration that can generate sufficient signal strength.
Note: The nonionic detergent Pluronic® F-127 is sometimes used to increase the aqueous solubility of Fluo-8® AM esters. A variety of Pluronic® F-127 solutions can be purchased from AAT Bioquest.

c) If your cells containing the organic anion-transports, probenecid (1–2.5 mM) or sulfinpyrazone (0.1–0.25 mM) may be added to the cell medium to reduce leakage of the de-esterified indicators.
Note: A variety of ReadiUse™ probenecid including water soluble sodium salt and stabilized solution can be purchased from AAT Bioquest.

d) Add equal volume of the dye working solution (from Step b or c) into your cell plate.

e) Incubate the dye-loading plate at a cell incubator or room temperature for 20 minutes to one hour.
Note: Decreasing the loading temperature might reduce the compartmentalization of the indictor.

f) Replace the dye working solution with HHBS or buffer of your choice (containing an anion transporter inhibitor, such as 2.5 mM probenecid, if applicable) to remove excess probes.

g) Run the experiments at Ex/Em = 490/525 nm

2. Measure Intracellular Calcium Responses: see figure 1.

IV. Use of Screen Quest™ Fluo-8 NW Calcium Assay Kits for HTS Applications

GPCR activation can be detected by direct measurement of the receptor mediated cAMP accumulation, or changes in intracellular Ca^{2+} concentration. GPCR targets that couple via Gq produce an increase in intracellular Ca^{2+} that can be measured using a combination of Fluo-8® reagents and a fluorescence microplate reader. The fluorescence imaging plate readers (such as, FLIPR™, FDSS or BMG NovoStar™) have a cooled CCD camera imaging system which collects the signal from each well of a microplate (both 96 and 384-well) simultaneously. These plate readers can read at sub-second intervals, which enables the kinetics of the response to be captured, and has an integrated pipettor that may be programmed for successive liquid additions. Besides their robust applications for GPCR targets, our Screen Quest™ Fluo-8 Calcium Assay Kits can be also used for characterizing calcium ion channels and screening calcium ion channel-targeted compounds.

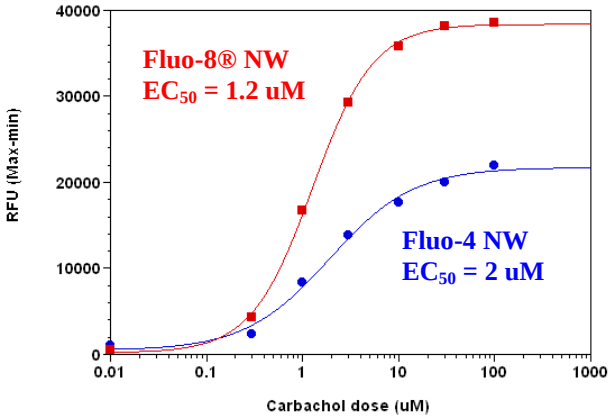

Figure 2. Carbachol Dose Response was measured in HEK-293 cells with Screen Quest™ Fluo-8 NW Assay kit and Fluo-4 NW Assay Kit**.** HEK-293 cells were seeded overnight at 40,000 cells/100 µL/well in a 96-well black wall/clear bottom costar plate. The growth medium was removed, and the cells were incubated with, respectively, 100 µL of the Screen Quest™ Fluo 8-NW calcium assay kit and Fluo-4 NW kit (according to the manufacturer's instructions) for 1 hour at room temperature. Carbachol (25µL/well) was added by NOVOstar (BMG LabTech) to achieve the final indicated concentrations. The EC_{50} of Fluo-8 NW is about 1.2 uM.

Compared to other commercial calcium assay kits that either based on Fluo-3 or Fluo-4, our Screen Quest™ Calcium Assay Kits have the following advantages for HTS applications:

- *Broad Applications:* work with both GPCR and calcium channel targets.
- *Convenient Spectral Wavelengths:* maximum excitation @ ~490 nm; maximum emission @ ~514 nm.
- *Flexible Dye Loading:* dye loading at room temperature (rather than 37 ºC required for Fluo-4 AM).
- *No Wash Required and No Quencher Interference with Your Targets.*
- *Robust Performance:* enable calcium assays that are impossible with Fluo-4 AM or Fluo-3 AM.
- *Strongest Signal Intensity:* 2 times brighter than that of Fluo-4 AM; 4 times brighter than that of Fluo-3 AM.

V. Use of Fluo-8® Salts

Calcium calibration can be carried out by measuring the fluorescence intensity of the salt form (25 to 50 µM in fluorescence microplate readers) of the indicators in solutions with precisely known free Ca^{2+} concentrations. Calibration solutions can be used based on 30 mM MOPS EGTA Ca^{2+} buffer. In general, water contains trace amount of calcium ion. It is highly recommended to use 30 mM MOPS + 100 mM KCl, pH 7.2 as buffer system. One can simply make a 0 and 39 µM calcium stock solutions as listed below, and these 2 solutions are used to make a serial solution of different Ca^{2+} concentrations

A. 0 µM calcium: 30 mM MOPS + 100 mM KCl, pH 7.2 buffer + 10 mM EGTA
B. 39 µM calcium: 30 mM MOPS + 100 mM KCl, pH 7.2 buffer + 10 mM EGTA + 10 mM $CaCl_2$

To determine either the free calcium concentration of a solution or the K_d of a single-wavelength calcium indicator, the following equation is used:

$$[Ca]_{free} = K_d[F - F_{min}]/F_{max} - F]$$

Where F is the fluorescence intensity of the indicator at a specific experimental calcium level, F_{min} is the fluorescence intensity in the absence of calcium and F_{max} is the fluorescence intensity of the calcium-saturated probe.

The dissociation constant (K_d) is a measure of the affinity of the probe for calcium. The calcium-binding and spectroscopic properties of fluorescent indicators vary quite significantly in cellular environments compared to calibration solutions. *In situ* response calibrations of intracellular indicators typically yield K_d values significantly higher than *in vitro* determinations. *In situ* calibrations are performed by exposing loaded cells to controlled Ca^{2+} buffers in the presence of ionophores such as A-23187, 4-bromo A-23187 and ionomycin. Alternatively, cell permeabilization agents such as digitonin or Triton® X-100 can be used to expose the indicator to the controlled Ca^{2+} levels of the extracellular medium. The K_d values of Fluo-8® reagents are listed in Table 1 for your reference.

VI. Conclusions

Because of the importance of Ca^{2+} in biology, numerous techniques/methods for analyzing the mechanisms of cellular and/or subcellular Ca^{2+} activity have been established. Unfortunately, however, there is no one best technique/method with which one can measure Ca^{2+}. Although each method for analyzing Ca^{2+}activity has certain advantages over the others, each also suffers drawbacks. With the outstanding properties described above, we believe that Fluo-8® calcium detection reagents and Screen Quest™ Fluo-8NW Calcium Assay Kits provide new powerful tools for intracellular calcium analysis and monitoring in a variety of biological systems in coupling with the rapid advance in fluorescence instrumentation.

As might have been predicted, the interests of many researchers shifted from Ca^{2+} analysis at the cellular level to the subcellular level. It has been found that Ca^{2+} is not even distributed throughout the whole cell and that intracellular heterogeneity of Ca^{2+} (such as Ca^{2+} waves and Ca^{2+} sparks) is observed in a variety of cells (e.g., oocyte, heart muscle cell, hepatocyte, and exocrine cell). With the advent of the confocal laser scanning microscope (CLSM) in the 1980s and advanced microplate readers in 2000s (such as FLIPR, FDSS and NOVOStar dedicated for intracellular Ca^{2+} detections), measurement of intracellular Ca^{2+} has accelerated significantly. Confocal laser scanning microscopy, and more recently multiphoton microscopy, allows the precise spatial and temporal analysis of intracellular Ca^{2+} activity at the subcellular level in addition to the measurement of its concentration.

Ordering: sales@aatbio.com; Tel: 800-990-8053 or 408-733-1055; Fax: 408-733-1304
Technical Support: support@aatbio.com; Tel: 408-733-1055

VII. Product List

Cat. #	Product Name	Unit Size
21080	Fluo-8®, AM *Cell-permeable*	1 mg
21081	Fluo-8®, AM *Cell-permeable*	5x50 µg
21082	Fluo-8®, AM *Cell-permeable*	10x50 µg
21083	Fluo-8®, AM *Cell-permeable*	20x50 µg
21086	Fluo-8®, sodium salt	1 mg
21087	Fluo-8®, potassium salt	1 mg
21088	Fluo-8®, sodium salt	10x50 µg
21089	Fluo-8®, potassium salt	10x50 µg
21090	Fluo-8H™, AM *Cell-permeable*	1 mg
21091	Fluo-8H™, AM *Cell-permeable*	10x50 µg
21095	Fluo-8H™, sodium salt	10x50 µg
21096	Fluo-8L™, AM *Cell-permeable*	1 mg
21097	Fluo-8L™, AM *Cell-permeable*	10x50 µg
21098	Fluo-8L™, sodium salt	10x50 µg
21099	Fluo-8L™, sodium salt	1 mg
21100	Fluo-8L™, potassium salt	10x50 µg
21101	Fluo-8L™, potassium salt	1 mg
21102	Fluo-8FF™, potassium salt	10x50 µg
21103	Fluo-8FF™, potassium salt	1 mg
21104	Fluo-8FF™, AM	10x50 µg
21105	Fluo-8FF™, AM	1 mg
36307	Screen Quest™ Fluo-8 NW Calcium Assay Kit *Medium Removal*	1 Plate
36308	Screen Quest™ Fluo-8 NW Calcium Assay Kit *Medium Removal*	10 Plates
36309	Screen Quest™ Fluo-8 NW Calcium Assay Kit *Medium Removal*	100 Plates
36314	Screen Quest™ Fluo-8 NW Calcium Assay Kit *1% FBS Growth Medium*	1 Plate
36315	Screen Quest™ Fluo-8 NW Calcium Assay Kit *1% FBS Growth Medium *	10 Plates
36316	Screen Quest™ Fluo-8 NW Calcium Assay Kit *1% FBS Growth Medium*	100 Plates

VIII. References

1. Alkhaldi, Jan Martinek , Brian Panicucci, Christophe Dardonville, Alena Zíkova, Harry P. de Koning. Trypanocidal action of bisphosphonium salts through a mitochondrial target in bloodstream form Trypanosoma brucei. International Journal for Parasitology: Drugs and Drug Resistance 6 (2016) 23e34.
2. Takahiro Shibata, Katsuhiro Takahashi, Yui Matsubara, Emi Inuzuka, Fumie Nakashima, Nobuaki Takahashi, Daisuke Kozai, Yasuo Mori & Koji Uchida. Identification of a prostaglandin D_2 metabolite as a neuritogenesis enhancer targeting the TRPV1 ion channel. Sci Rep. 2016; 6: 21261. Published online 2016 Feb 16. doi: 10.1038/srep21261.
3. Boris Gourévitchh, Jun Cai, Nicholas Mellen. Cellular and network-level adaptations to in utero methadone exposure along the ventral respiratory column in the neonate rat**.** Experimental Neurology**.** Available online 20 March 2016.
4. Aditya J. Desai, Maoqing Dong, Laurence J. Miller**.** Beneficial effects of β-sitosterol on type 1 cholecystokinin receptor dysfunction induced by elevated membrane cholesterol**.** Clinical Nutrition**.** Available online 15 March 2016.
5. Wiktor S. Phillips, Mikkel Herly, Christopher A. Del Negro, and Jens C. Rekling . Organotypic slice cultures containing the preBötzinger complex generate respiratory-like rhythms**.** *J Neurophysiol.* 2016; 115:1063-1070.
6. Jin-Feng Zhao, Song-Kun Shyue, and Tzong-Shyuan Lee. Excess Nitric Oxide Activates TRPV1-Ca^{2+}-Calpain Signaling and Promotes PEST-dependent Degradation of Liver X Receptor α**.** Int J Biol Sci. 2016; 12(1): 18–29. doi: 10.7150/ijbs.13549.
7. Robert A. Volkmann, Christopher M. Fanger, David R. Anderson, Venkata Ramana Sirivolu, Kathy Paschetto, Earl Gordon, Caterina Virginio, Melanie Gleyzes, Bruno Buisson, Esther Steidl, Susanna B. Mierau, Michela Fagiolini, Frank S. Menniti . MPX-004 and MPX-007: New Pharmacological Tools to Study the Physiology of NMDA Receptors Containing the GluN2A Subunit**.** Plos one. Published: February 1, 2016. http://dx.doi.org/10.1371/journal.pone.0148129.
8. Retsu Mitsui , Hikaru Hashitani. Mechanisms underlying spontaneous constrictions of postcapillary venules in the rat stomach**.** Pflügers Archiv - European Journal of Physiology, Muscle Physiology, February 2016, Volume 468, Issue 2, pp 279-291.
9. Masae Ishiguro, Alan Okada, Kiyofumi Asai, Kiyohide Kojima and Hidechika Okada. Stimulation of neuronal cells by culture supernatant of T lymphocytes triggered by anti-CD3 mAb followed by propagation in the presence of interleukin-2. Microbiology and Immunology. 14 JAN 2016. DOI: 10.1111/1348-0421.12346.
10. Edyta Gendaszewska-Darmach , Marcin Szustak. Thymidine 5'-*O*-monophosphorothioate induces HeLa cell migration by activation of the P2Y6 receptor. Purinergic Signalling. pp 1-11. First online: 08 January 2016.

Ordering: sales@aatbio.com; Tel: 800-990-8053 or 408-733-1055; Fax: 408-733-1304
Technical Support: support@aatbio.com; Tel: 408-733-1055

11. Lina Zhou, Wei Cheng, Hongzhou Hou, Renyi Peng, Na Hai, Zhiyuan Bian, Chengjin Jiao, Chongying Wang . Antioxidative Responses and Morpho-anatomical Alterations for Coping with Flood-Induced Hypoxic Stress in Grass Pea (Lathyrus sativus L.) in Comparison with Pea (Pisum sativum)**.** Journal of Plant Growth Regulation. pp 1-11. First online: 02 February 2016.
12. Francesco A. Mistretta, Andrea Russo, Fabio Castiglione, Arianna Bettiga,Giorgia Colciago, Francesco Montorsi, Laura Brandolini, Andrea Aramini,Gianluca Bianchini, Marcello Allegretti, Silvia Bovolenta, Roberto Russo, Fabio Benigni, and Petter Hedlund. DFL23448, A Novel Transient Receptor Potential Melastin 8–Selective Ion Channel Antagonist, Modifies Bladder Function and Reduces Bladder Overactivity in Awake Rats. Published online before printNovember 6, 2015, doi:10.1124/jpet.115.228684JPET January 2016 vol. 356no. 1 200-211.
13. Daniele Guido, Nicolas Demaurex, Paula Nunes. Junctate boosts phagocytosis by recruiting endoplasmic reticulum Ca^{2+}stores near phagosomes. J Cell Sci 2015 128: 4074-4082; doi: 10.1242/jcs.172510.
14. J.T. Lock, I. Parker, I.F. Smith, A comparison of fluorescent Ca2+ indicators for imaging local Ca2+ signals in cultured cells, Cell Calcium (2015) October, http://dx.doi.org/10.1016/j.ceca.2015.10.003.
15. L Miller, DS Steele, DJ Greensmith, G Hart, H Dobrzynski, and MR Boyett**.** 8 Stimulation of calcium sparks in both sino – atrial node and ventricular myocytes. Heart, Nov 2015; 101: A3.
16. Dan-yang Guo, De-wen Li, Meng-meng Ning, Xiang-yu Dang, Li-na Zhang, Li-min Zeng, You-hong Hu, Ying Leng. Yhhu4488, a novel GPR40 agonist, promotes GLP-1 secretion and exerts anti-diabetic effect in rodent models**.** Biochemical and Biophysical Research Communications**.** Volume 466, Issue 4, 30 October 2015, Pages 740–747.
17. Aditya J. Desai, Polo C. H. Lam, Andrew Orry, Ruben Abagyan, Arthur Christopoulos, Patrick M. Sexton, andLaurence J. Miller. Molecular Mechanism of Action of Triazolobenzodiazepinone Agonists of the Type 1 Cholecystokinin Receptor. Possible Cooperativity across the Receptor Homodimeric Complex. *J. Med. Chem.*, 2015, *58* (24), 9562–9577. DOI: 10.1021/acs.jmedchem.5b01110.
18. Nicola A. Irvine, Karen A. Lillycrop, Barbara Fielding, Christopher Torrens, Mark A. Hanson, Graham C. Burdge. Polyunsaturated fatty acid biosynthesis is involved in phenylephrine-mediated calcium release in vascular smooth muscle cells**.** Prostaglandins, Leukotrienes and Essential Fatty Acids (PLEFA)**.** Volume 101, October 2015, Pages 31–39.
19. Junichiro Takaya, Kazuhiro Mio, Takuya Shiraishi, Tatsuki Kurokawa, Shinya Otsuka, Yasuo Mori, and Motonari Uesugi. A Potent and Site-Selective Agonist of TRPA1. *J. Am. Chem. Soc.*, 2015, *137* (50), pp 15859–15864. DOI: 10.1021/jacs.5b10162.
20. Mads Harsløf, Felix C. Müller, Julie Rohrberg, Jens C. Rekling. Fast neuronal labeling in live tissue using a biocytin conjugated fluorescent probe**.** Journal of Neuroscience Methods**.** Volume 253, 30 September 2015, Pages 101–109.
21. Karin P. Hammer, Senka Ljubojevic, Crystal M. Ripplinger, Burkert M. Pieske,Donald M. Bers. Cardiac myocyte alternans in intact heart: Influence of cell–cell coupling and β-adrenergic stimulation**.** Journal of Molecular and Cellular Cardiology**.** Volume 84, July 2015, Pages 1–9.
22. Yilu Zhou, Miri Park, Enoch Cheung, Liyun Wang, X. Lucas Lu. The effect of chemically defined medium on spontaneous calcium signaling of *in situ* chondrocytes during long-term culture. Volume 48, Issue 6, 13 April 2015, Pages 990–996.
23. Régis Stentz, Samantha Osborne, Nikki Horn, Arthur W.H. Li, Isabelle Hautefort, Roy Bongaerts,Marine Rouyer, Paul Bailey, Stephen B. Shears, Andrew M. Hemmings, Charles A. Brearley , Simon R. Carding. A Bacterial Homolog of a Eukaryotic Inositol Phosphate Signaling Enzyme Mediates Cross-kingdom Dialog in the Mammalian Gut. Cell reports Volume 6, Issue 4, 27 February 2014, Pages 646–656. doi:10.1016/j.celrep.2014.01.021
24. Aditya J. Desai, Maoqing Dong, Kaleeckal G. Harikumar, Laurence J. Miller. Miller. Impact of ursodeoxycholic acid on a CCK1R cholesterol-binding site may contribute to its positive effects in digestive function. American Journal of Physiology - Gastrointestinal and Liver Physiology Published 1 September 2015 Vol. 309 no. 5, G377-G386 DOI: 10.1152/ajpgi.00173.2015.
25. Emery Smith, Peter Chase, Colleen M. Niswender, Thomas J. Utley, Douglas J. Sheffler, Meredith J. Noetzel, Atin Lamsal, Michael R. Wood, P. Jeffrey Conn, Craig W. Lindsley, Franck Madoux, Mary Acosta, Louis Scampavia, Timothy Spicer, and Peter Hodder. Application of Parallel Multiparametric Cell-Based FLIPR Detection Assays for the Identification of Modulators of the Muscarinic Acetylcholine Receptor 4 (M_4). *J Biomol Screen.* 2015; 20:858-868. doi:10.1177/1087057115581770.
26. Krähling, Anke Miriam, Luis Alvarez, Katharina Debowski, Qui Van, Monika Gunkel, Stephan Irsen, Ashraf Al-Amoudi et al. "CRIS—a novel CAMP-binding protein controlling spermiogenesis and the development of flagellar bending."*PLoS genetics* 9, no. 12 (2013): e1003960.
27. Pengcheng Liu, Hong-Juan Peng, and Jinsong Zhu. Juvenile hormone-activated phospholipase C pathway enhances transcriptional activation by the methoprene-tolerant protein. *PNAS.* 2015; 112:E1871-E1879.
28. Mako Kurogi, Yasushi Kawai, Katsuhiro Nagatomo, Michihiro Tateyama, Yoshihiro Kubo, and Osamu Saitoh. Auto-oxidation Products of Epigallocatechin Gallate Activate TRPA1 and TRPV1 in Sensory Neurons. *Chem Senses.* 2015; 40:27-46.
29. Nasse, Jason S. "A novel slice preparation to study medullary oromotor and autonomic circuits in vitro." *Journal of neuroscience methods* 237 (2014): 41-53.
30. Hiroya Takada, Kishio Furuya, and Masahiro Sokabe. Mechanosensitive ATP release from hemichannels and Ca^{2+} influx through TRPC6 accelerate wound closure in keratinocytes. *J. Cell Sci.* 2014; 127:4159-4171.
31. Shusei Mizushima, Gen Hiyama, Kogiku Shiba, Kazuo Inaba, Hideo Dohra, Tamao Ono, Kiyoshi Shimada, and Tomohiro Sasanami. The birth of quail chicks after intracytoplasmic sperm injection**.** *Development.* 2014; 141:3799-3806.
32. Elizabeth M Zipprer, McKinzie Neggers, Ambuj Kushwaha, Kempaiah Rayavara and Sanjay A Desai. A kinetic fluorescence assay reveals unusual features of Ca++ uptake in Plasmodium falciparum-infected erythrocytes. Malaria Journal 2014, 13:184.
33. Gourévitch B, Mellen N. The preBötzinger complex as a hub for network activity along the ventral respiratory column in the neonate rat. Neuroimage. 2014 Sep; 98:460-74. doi: 10.1016/j.neuroimage.2014.04.073. Epub 2014.
34. Aditya J. Desai, Kaleeckal G. Harikumar, and Laurence J. Miller. A Type 1 Cholecystokinin Receptor Mutant That Mimics the Dysfunction Observed for Wild Type Receptor in a High Cholesterol Environment. *J. Biol. Chem.* 2014; 289:18314-18326.
35. D Warszta and A H Guse. A view from inside: simultaneous live cell imaging of free SR and cytosolic calcium concentrations. Cardiovascular Research Supplements (2014) 103, S57–S94.

36. R. Benjamin Free, Lani S. Chun, Amy E. Moritz, Brittney N. Miller, Trevor B. Doyle, Jennie L. Conroy, Adrian Padron, Julie A. Meade, Jingbo Xiao, Xin Hu, Andrés E. Dulcey, Yang Han, Lihua Duan, Steve Titus, Melanie Bryant-Genevier, Elena Barnaeva, Marc Ferrer, Jonathan A. Javitch, Thijs Beuming, Lei Shi, Noel T. Southall, Juan J. Marugan, and David R. Sibley. Discovery and Characterization of a G Protein–Biased Agonist That Inhibits b-Arrestin Recruitment to the D2 Dopamine Receptor. Mol Pharmacol 86:96–105, 2014, doi /10.1124/mol.113.090563.
37. Shiro Nakamura, Kiyomi Nakayama, Ayako Mochizuki, Fumihiko Sato, Tahsinul Haque, Atsushi Yoshida, and Tomio Inoue. Electrophysiological and morphological properties of rat supratrigeminal premotor neurons targeting the trigeminal motor nucleus. *J Neurophysiol.* 2014; 111:1770-1782.
38. Sanjeev Kumar Mahto, Janna Tenenbaum-Katan, Ayala Greenblum, Barbara Rothen-Rutishauser, and Josué Sznitman. Microfluidic shear stress-regulated surfactant secretion in alveolar epithelial type II cells in vitro *Am J Physiol Lung Cell Mol Physiol.* 2014; 306:L672-L683.
39. Da Jing, Andrew D. Baik, X. Lucas Lu, Bin Zhou, Xiaohan Lai, Liyun Wang, Erping Luo, and X. Edward Guo. *In situ* intracellular calcium oscillations in osteocytes in intact mouse long bones under dynamic mechanical loading. *FASEB J.* 2014; 28:1582-1592.
40. Stefka Mincheva-Tasheva, Elia Obis, Jordi Tamarit, and Joaquim Ros. Apoptotic cell death and altered calcium homeostasis caused by frataxin depletion in dorsal root ganglia neurons can be prevented by BH4 domain of Bcl-x_L protein. *Hum. Mol. Genet.* 2014; 23:1829-1841.
41. Mathias Kølvraa, Felix C. Müller, Henrik Jahnsen, and Jens C. Rekling. Mechanisms contributing to cluster formation in the inferior olivary nucleus in brainstem slices from postnatal mice. *J. Physiol.* 2014; 592:33-47.
42. Stefka Mincheva-Tasheva, Elia Obis, Jordi Tamarit, and Joaquim Ros. Apoptotic cell death and altered calcium homeostasis caused by frataxin depletion in dorsal root ganglia neurons can be prevented by BH4 domain of Bcl-x_L protein. Hum. Mol. Genet**.,** Nov 2013; 10.1093/hmg/ddt576.
43. Kenichi Sasaki, Takeru Makiyama, Yoshinori Yoshida, Hideki Itoh, Mihoko Kawamura, Naokata Sumitomo, Masaru Miura, Takeshi Harita, Suguru Nishiuchi, Mamoru Hayano, Yuta Yamamoto, Yimin Wuriyanghai, Jiarong Chen, Tsukasa Kamakura, Tetsuhisa Hattori, Seiko Ohno, Minoru Horie, Shinya Yamanaka, and Takeshi Kimura. Modeling Catecholaminergic Polymorphic Ventricular Tachycardia Using Human Induced Pluripotent Stem Cells: A Promising Tool for Drug Discovery. Circulation, Nov 2013; 128: A14419.
44. Erwann Rousseau, Patrick P. Michel, and Etienne C. Hirsch. The Iron-Binding Protein Lactoferrin Protects Vulnerable Dopamine Neurons from Degeneration by Preserving Mitochondrial Calcium Homeostasis**.** Mol. Pharmacol., Dec 2013; 84: 888 - 898.
45. Vladimir N. Podust, Bee-Cheng Sim, Dharti Kothari, Lana Henthorn, Chen Gu, Chia-wei Wang, Bryant McLaughlin, and Volker Schellenberger. Extension of *in vivo* half-life of biologically active peptides via chemical conjugation to XTEN protein polymer. Protein Eng. Des. Sel., Nov 2013; 26: 743 - 753.
46. Emily M. Lynes, Arun Raturi, Marina Shenkman, Carolina Ortiz Sandoval, Megan C. Yap, Jiahui Wu, Aleksandra Janowicz, Nathan Myhill, Matthew D. Benson, Robert E. Campbell, Luc G. Berthiaume, Gerardo Z. Lederkremer, and Thomas Simmen. Palmitoylation is the switch that assigns calnexin to quality control or ER Ca^{2+} signaling. J. Cell Sci., Sep 2013; 126: 3893 - 3903.
47. Lani S. Chun, R. Benjamin Free, Trevor B. Doyle, Xi-Ping Huang, Michele L. Rankin, and David R. Sibley D_1-D_2 Dopamine Receptor Synergy Promotes Calcium Signaling via Multiple Mechanisms Mol. Pharmacol., Aug 2013; **8**4: 190 - 200.
48. Kaleeckal G. Harikumar, Erin E. Cawston, Polo C. H. Lam, Achyut Patil, Andrew Orry, Brad R. Henke, Ruben Abagyan, Arthur Christopoulos, Patrick M. Sexton, and Laurence J. Miller. Molecular Basis for Benzodiazepine Agonist Action at the Type 1 Cholecystokinin Receptor J. Biol. Chem., Jul 2013; 288: 21082 - 21095.
49. Annika Thorsell, Jenica D. Tapocik, Ke Liu, Michelle Zook, Lauren Bell, Meghan Flanigan, Samarjit Patnaik, Juan Marugan, Ruslan Damadzic, Seameen J. Dehdashti, Melanie L. Schwandt, Noel Southall, Christopher P. Austin, Robert Eskay, Roberto Ciccocioppo, Wei Zheng, and Markus Heilig. A Novel Brain Penetrant NPS Receptor Antagonist, NCGC00185684, Blocks Alcohol-Induced ERK-Phosphorylation in the Central Amygdala and Decreases Operant Alcohol Self-Administration in Rats. J. Neurosci., Jun 2013; 33: 10132 - 10142.
50. Xueying Wang, John A. Hayes, Maria Cristina D. Picardo, and Christopher A. Del Negro. Automated cell-specific laser detection and ablation of neural circuits in neonatal brain tissue J. Physiol., May 2013; 591: 2393 – 2401.
51. Ryszard Grygorczyk, Kishio Furuya, and Masahiro Sokabe. Imaging and characterization of stretch-induced ATP release from alveolar A549 cells. J. Physiol., Mar 2013; 591: 1195 - 1215.
52. Hirofumi Watari, Amanda J. Tose, and Martha M. Bosma. Hyperpolarization of resting membrane potential causes retraction of spontaneous transients during mouse embryonic circuit development**.** J. Physiol., Feb 2013; 591: 973 - 983.
53. Shekher Mohan, Shuh Narumiya, and Sylvain Dore. PGE2 EP1 Receptor Blockade Prevents Hemin-Induced Neurotoxicity In An In Vitro Model of Intracerebral Hemorrhage Stroke, Feb 2013; 44: AWP299.
54. Houssein S. Abdou, Gabrielle Villeneuve, and Jacques J. Tremblay. The Calcium Signaling Pathway Regulates Leydig Cell Steroidogenesis through a Transcriptional Cascade Involving the Nuclear Receptor NR4A1 and the Steroidogenic Acute Regulatory Protein. Endocrinology, Jan 2013; 154: 511 - 520.
55. P. Senbagavalli, J. Nancy Hilda, V. D. Ramanathan, V. Kumaraswami, Thomas B. Nutman, and Subash Babu. Immune Complexes Isolated from Patients with Pulmonary Tuberculosis Modulate the Activation and Function of Normal Granulocytes Clin. Vaccine Immunol., Dec 2012; 19: 1965 - 1971.
56. Mikihito Kajiya, Isao Ichimonji, Christine Min, Tongbo Zhu, Jun-O Jin, Qing Yu, Soulafa A. Almazrooa, Seunghee Cha, and Toshihisa Kawai. Muscarinic Type 3 Receptor Induces Cytoprotective Signaling in Salivary Gland Cells through Epidermal Growth Factor Receptor Transactivation Mol. Pharmacol., Jul 2012; 82: 115 - 124.
57. Wen Fu, Araya Ruangkittisakul, David MacTavish, Jenny Y. Shi, Klaus Ballanyi, and Jack H. Jhamandas. Amyloid β (Aβ) Peptide Directly Activates Amylin-3 Receptor Subtype by Triggering Multiple Intracellular Signaling Pathways J. Biol. Chem., May 2012; 287: 18820 - 18830.

58. Soichi Watanabe, Andre P. Seale, E. Gordon Grau, and Toyoji Kaneko. Stretch-activated cation channel TRPV4 mediates hyposmotically induced prolactin release from prolactin cells of mozambique tilapia*Oreochromis mossambicus*. *Am J Physiol Regulatory Integrative Comp Physiol.* 2012; 302: R1004 - R1011.
59. Mako Kurogi, Megumi Miyashita, Yuri Emoto, Yoshihiro Kubo, and Osamu Saitoh. Green Tea Polyphenol Epigallocatechin Gallate Activates TRPA1 in an Intestinal Enteroendocrine Cell Line, STC-1. *Chem Senses* 2012; 37: 167 - 177.
60. Hideki Hayashi, Yuko Eguchi, Yuko Fukuchi-Nakaishi, Motohiro Takeya, Naomi Nakagata, Kohichi Tanaka, Jean E. Vance, and Hidenobu Tanihara. A Potential Neuroprotective Role of Apolipoprotein E-containing Lipoproteins through Low Density Lipoprotein Receptor-related Protein 1 in Normal Tension Glaucoma. *J. Biol. Chem*., 2012; 287: 25395 – 25406.
61. Jens C. Rekling, Kristian H. R. Jensen, and Henrik Jahnsen. Spontaneous cluster activity in the inferior olivary nucleus in brainstem slices from postnatal mice. *J. Physiol.* 2012; 590: 1547 - 1562.
62. Marc Aurel Busche, Xiaowei Chen, Horst A. Henning, Julia Reichwald, Matthias Staufenbiel, Bert Sakmann, and Arthur Konnerth. Critical role of soluble amyloid-β for early hippocampal hyperactivity in a mouse model of Alzheimer's disease. *PNAS* 2012; 109: 8740 - 8745.
63. John A. Hayes, Xueying Wang, and Christopher A. Del Negro Cumulative lesioning of respiratory interneurons disrupts and precludes motor rhythms in vitro. *PNAS*, 2012; 109: 8286 - 8291.
64. Calcium Signaling edited by Md. Shahidul Islam, 2012.
65. Shaona Acharjee, Yu Zhu, Ferdinand Maingat, Carlos Pardo, Klaus Ballanyi, Morley D. Hollenberg, and Christopher Power. Proteinase-activated receptor-1 mediates dorsal root ganglion neuronal degeneration in HIV/AIDS. *Brain* 2011; 134: 3209 - 3221.
66. Yasuto Yamaguchi, Xiao-Yan Du, Lei Zhao, John Morser, and Lawrence L. K. Leung. Proteolytic Cleavage of Chemerin Protein Is Necessary for Activation to the Active Form, Chem157S, Which Functions as a Signaling Molecule in Glioblastoma. *J. Biol. Chem.* 2011; 286: 39510 - 39519.
67. Masato Maesako, Kengo Uemura, Akira Kuzuya, Kazuki Sasaki, Megumi Asada, Kiwamu Watanabe, Koichi Ando, Masakazu Kubota, Takeshi Kihara, and Ayae Kinoshita. Presenilin Regulates Insulin Signaling via a γ-Secretase-independent Mechanism. *J. Biol. Chem.*, 2011; 286: 25309 - 25316.
68. Wei-Wei Shen, Maud Frieden, and Nicolas Demaurex. Local Cytosolic Ca^{2+} Elevations Are Required for Stromal Interaction Molecule 1 (STIM1) De-oligomerization and Termination of Store-operated Ca^{2+} Entry. *J. Biol. Chem.* 2011; 286: 36448 - 36459.
69. André M. Deslauriers, Amir Afkhami-Goli, Amber M. Paul, Rakesh K. Bhat, Shaona Acharjee, Kristofor K. Ellestad, Farshid Noorbakhsh, Marek Michalak, and Christopher Power**.** Neuroinflammation and Endoplasmic Reticulum Stress Are Coregulated by Crocin To Prevent Demyelination and Neurodegeneration. *J. Immunol.* 2011; 187: 4788 - 4799.
70. Man Hagiyama, Tadahide Furuno, Yoichiroh Hosokawa, Takanori Iino, Takeshi Ito, Takao Inoue, Mamoru Nakanishi, Yoshinori Murakami, and Akihiko Ito**.** Enhanced Nerve–Mast Cell Interaction by a Neuronal Short Isoform of Cell Adhesion Molecule-1. *J. Immunol.* 2011; 186: 5983 - 5992.
71. Christopher A. Del Negro, John A. Hayes, and Jens C. Rekling**.** Dendritic Calcium Activity Precedes Inspiratory Bursts in preBötzinger Complex Neurons. *J. Neurosci.* 2011; 31: 1017 - 1022.
72. Karin Persson and Jens C. Rekling**.** Population calcium imaging of spontaneous respiratory and novel motor activity in the facial nucleus and ventral brainstem in newborn mice. *J. Physiol.* 2011; 589: 2543 - 2558.
73. Nicholas B. Last, Elizabeth Rhoades, and Andrew D. Miranker. Islet amyloid polypeptide demonstrates a persistent capacity to disrupt membrane integrity. *PNAS* 2011; 108: 9460 - 9465.
74. Ferdinand Maingat, Brendan Halloran, Shaona Acharjee, Guido van Marle, Deirdre Church, M. John Gill, Richard R. E. Uwiera, Eric A. Cohen, Jon Meddings, Karen Madsen, and Christopher Power**.** Inflammation and epithelial cell injury in AIDS enteropathy: involvement of endoplasmic reticulum stress. *FASEB J.* 2011; 25: 2211 - 2220.
75. Silke Meister, Benjamin Frey, Veronika R. Lang, Udo S. Gaipl, Georg Schett, Ursula Schlötzer-Schrehardt and Reinhard E. Voll. Verapamil Enhances Endoplasmic Reticulum Stress and Cell Death Induced by Proteasome. Inhibition in Myeloma Cells. Neoplasia Volume 12 Number 7 July 2010 pp. 550–561.
76. Satoru Torii, Kentaro Kobayashi, Masayuki Takahashi, Kasumi Katahira, Kenji Goryo, Natsuki Matsushita, Ken-ichi Yasumoto, Yoshiaki Fujii-Kuriyama, and Kazuhiro Sogawa**.** Magnesium Deficiency Causes Loss of Response to Intermittent Hypoxia in Paraganglion Cells. *J. Biol. Chem.* 2009; 284: 19077 - 19089.
77. Takako Saito, Kogiku Shiba, Kazuo Inaba, Lixy Yamada, and Hitoshi Sawada. Self-incompatibility response induced by calcium increase in sperm of the ascidian *Ciona intestinalis*. *PNAS* 2012; 109: 4158 - 4162.
78. Yohei Okubo, Hiroshi Sekiya, Shigeyuki Namiki, Hirokazu Sakamoto, Sho Iinuma, Miwako Yamasaki, Masahiko Watanabe, Kenzo Hirose, and Masamitsu Iino**.** Imaging extrasynaptic glutamate dynamics in the brain. *PNAS* 2010; 107: 6526 - 6531.
79. Katsutoshi Mizuno, Kogiku Shiba, Masahiko Okai, Yusuke Takahashi, Yuji Shitaka, Kazuhiro Oiwa, Masaru Tanokura, and Kazuo Inaba. Calaxin drives sperm chemotaxis by Ca^{2+}-mediated direct modulation of a dynein motor. PNAS, Dec 2012; 109: 20497 - 20502.
80. Nicholas M. Mellen and Deepak Mishra. Functional Anatomical Evidence for Respiratory Rhythmogenic Function of Endogenous Bursters in Rat Medulla**.** *J. Neurosci.* 2010; 30: 8383 - 8392.